Comparison of the acceleration, length, and velocity forms of the dipole operator in photoionization calculations*

Michael S. Pindzola and Hugh P. Kelly
Department of Physics, University of Virginia, Charlottesville, Virginia 22901
(Received 31 March 1975)

The acceleration, length, and velocity forms of the dipole operator are used to calculate the subshell photoionization cross sections in argon. First-order electron correlation corrections to the Hartree-Fock approximation are obtained through the use of many-body perturbation theory. For low-energy transitions the acceleration form of the operator is found to give very large errors in the Hartree-Fock approximation as compared to the length and velocity operators. Correlation effects for the three operator formulations are found to be quite different.

In recent years numerous calculations have been made on various photoabsorption processes in atoms.[1-4] Typically, bound-free absorption results of Hartree-Fock accuracy or greater have been reported[3] using the length and velocity forms of the dipole operator. A few calculations have, however, been carried out[5,6] using the acceleration, length, and velocity forms. In general, the acceleration form has been regarded[7] as being valid for only high-energy transitions, but very few tests[8] have been made with it for bound-free absorption rates in complex atoms. In calculating free-free absorption cross sections the acceleration form has been used quite frequently.[4] The acceleration form seems more convenient[9] than the length and velocity forms[10] because of the immediate convergence of the continuum-continuum dipole-matrix elements found in free-free scattering. In order to get some feeling for the range of validity of the acceleration form, we examine in this paper the different subshell photoionization cross sections in argon calculated using all three forms. Many-body perturbation theory is used to obtain the first-order correlation corrections to the Hartree-Fock approximation.

The photoionization cross section for an atom may be calculated[11] by using the many-body perturbation theory of Brueckner[12] and Goldstone.[13] The Hamiltonian of the atom (in atomic units) is given by

$$H = H_0 + H_1, \tag{1}$$

where

$$H_0 = \sum_{i=1}^{N} \left(-\tfrac{1}{2}\nabla_i^2 - Z/r_i + V_i\right) \tag{2}$$

and

$$H_1 = \sum_{i<j=1}^{N} v_{ij} - \sum_{i=1}^{N} V_i . \tag{3}$$

The single-particle potential V_i may be taken[14] to be a spherically symmetric Hartree-Fock V^{N-1}-type potential corresponding to an LS-coupled many-particle state, while v_{ij} is the Coulomb interaction between electrons. The solution Φ_k of the Schrödinger equation $H_0\Phi_k = E_k\Phi_k$ may be expressed as a linear combination of determinants formed from the single-particle (bound and continuum) solutions ϕ_k of

$$\left[-\tfrac{1}{2}\nabla^2 - (Z/r) + V\right]\phi_k = \epsilon_k\phi_k , \tag{4}$$

where

$$\langle \vec{r} \,|\, k l m_l m_s\rangle = R(k, l; r) Y_{lm}(\theta, \phi)\chi_s(m_s). \tag{5}$$

$Y_{lm}(\theta, \phi)$ is a spherical harmonic, $\chi_s(m_s)$ is a spin function, and the radial continuum states are normalized according to

$$R(k, l; r) \to \sin\left[kr + \delta_l + (q/k)\ln(2kr) - \tfrac{1}{2}l\pi\right]/r \quad \text{as } r \to \infty, \tag{6}$$

where $V(r) \to q/r$.

The atom–radiation-field interaction Hamiltonian along with H_1 of Eq. (3) serve as the perturbation in a linked-cluster expansion for the photoionization cross section $\sigma(\omega)$. It can be shown[15] in the dipole approximation using the continuum normalization of Eq. (6) that

$$\sigma(\omega) = (8\pi\mathcal{R}/\omega kc)\,|M|^2, \tag{7}$$

where in the length L, velocity V, and acceleration A forms[16]

$$M_L = \omega\,\langle \Psi_k \,|\, \sum_{i=1}^{N} \hat{\epsilon}\cdot\vec{r}_i \,|\, \Psi_0\rangle , \tag{8}$$

$$M_V = \langle \Psi_k \,|\, \sum_{i=1}^{N} \hat{\epsilon}\cdot\nabla_i \,|\, \Psi_0\rangle , \tag{9}$$

and

$$M_A = \frac{Z}{\omega}\,\langle \Psi_k \,|\, \sum_{i=1}^{N} \frac{\hat{\epsilon}\cdot\vec{r}_i}{r_i^3} \,|\, \Psi_0\rangle . \tag{10}$$

In Eqs. (7)–(10) the Ψ_0 and Ψ_k are exact many-particle ground and continuum states, ω is the frequency of the radiation, and k is the momentum of the ionized electron. The normalization factor $\mathfrak{N}$ accounts for the fact that $\langle \Psi_0 | \Psi_0 \rangle \neq 1$ if Ψ_0 is calculated by a perturbation expansion. For photoabsorption processes in argon $\mathfrak{N}$ was found[17] to be very close to unity. For exact atomic wave functions the three forms of M are of course equivalent, but since perturbation theory is used to evaluate them they may differ by significant amounts in lowest order. The acceleration form M_A of Eq. (10) can also be written in a form involving the gradient of the atomic potential. Certain correlation effects may be included by adding a polarization potential term to a suitable central-field atomic potential[9].

Many-body techniques developed in previous photoionization calculations[11] are used to evaluate Eqs. (7)–(10). The lowest order for M is represented by the diagram of Fig. 1(a). The solid dot indicates an interaction with the radiation field. The use of Fig. 1(a) alone in Eqs. (7)–(10) yields the Hartree-Fock approximation to the photoionization cross section, provided V of Eq. (4) is the Hartree-Fock potential. Diagrams of first order in the Coulomb correlations are shown in Figs. 1(b) and 1(c). The dashed lines not ending in dots represent Coulomb interactions. There are also exchange diagrams corresponding to the direct diagrams of Figs. 1(b) and 1(c).

By the use of Eq. (5) for the single-particle states, each diagram may be analyzed into its various angular-momentum excitation components. For example, the notation $[3p \rightarrow kd,\ 2p \rightarrow n's,\ k's]$ may be used to describe that particular component of the first-order diagrams in which a $3p$ electron of argon is ionized by interacting with a virtual transition of a $2p$ electron to an excited $l=0$ orbital. Each excitation component of each diagram involves an angular summation over m_l and m_s as well as radial integrations over the Coulomb and radiation field interactions. Singularities in the energy denominators of the diagrams are treated according to $(D+i\epsilon)^{-1} = PD^{-1} - i\pi\delta(D)$.[16] The denominator of Fig. 1(c) and its corresponding exchange will vanish for certain values of $\omega = \epsilon_{n'} - \epsilon_q$ where n' is a bound excited state. These are autoionization resonances. By summing certain higher-order diagrams[17] a half-width and level shift can be introduced in the denominator to remove the pole.

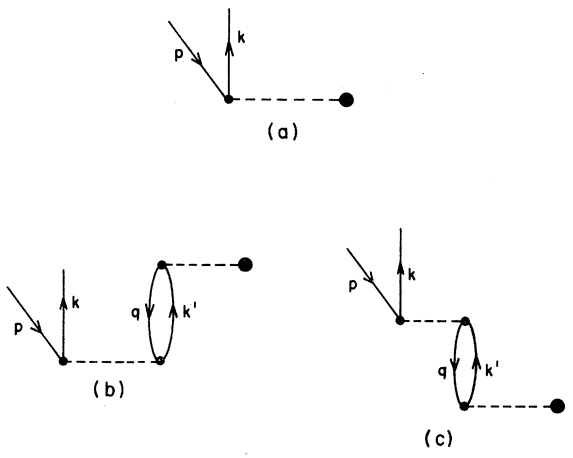

FIG. 1. Diagrams occurring in the perturbation expansion for the matrix element. Solid dots indicate interaction with the radiation field; dashed lines not ending in dots represent Coulomb interactions. Diagram (a) gives the lowest-order Hartree-Fock result when the Hartree-Fock potential V is used in Eq. (4). There are also exchange diagrams associated with the first-order Coulomb correlation diagrams shown in (b) and (c).

The photoionization cross sections for the $3p$, $3s$, and $2p$ subshells of argon were calculated using the length, velocity, and acceleration forms of $\sigma(\omega)$ given by Eqs. (7)–(10). The single-particle energies used in evaluating the diagrams of Fig. 1 are taken from the experimental values given by Moore.[18] Complete sets of bound and continuum radial functions are generated using Eq. (4) for the many-particle configurations $(3p)^5kd\ ^1P$, $(3p)^5ks\ ^1P$, $(3s)(3p)^6kp\ ^1P$, and $(2p)^5(3s)^2(3p)^6kd\ ^1P$. The Silverstone[19]-Huzinaga[20] potential was used when necessary to ensure orthogonality between the excited and core states.

The $3p \rightarrow kd\ ^1P$ photoionization cross section in the lowest-order Hartree-Fock approximation is given in Fig. 2 by the curves labeled HFL, HFV, and HFA. In previous work[17] the Hartree-Fock length (HFL) and velocity (HFV) curves were found to bracket the experimental results.[21] By including electron correlations through higher-order diagrams, the calculated values can be brought[17] into excellent agreement with experiment using the length and velocity forms. The acceleration curve (HFA), however, lies an order of magnitude above the HFL and HFV results. It is interesting to compare the effects of the various subshell components of the first-order correlation diagrams on the lowest-order HFL, HFV, and HFA results. Table I compares the three methods for the $3p \rightarrow kd\ ^1P$ cross section at $\omega = 20.060$ eV. Inner-shell correlation effects are seen to play a very important role when using the acceleration form. This is not surprising[16] since the r^{-2} factor in the matrix element of Eq. (10) tends to emphasize the small-r range of the wave functions. The curves labeled Ans ($n = 1, 2, 3$) or Anp ($n = 2, 3$) in Fig. 2 show how the individual subshell correlation com-

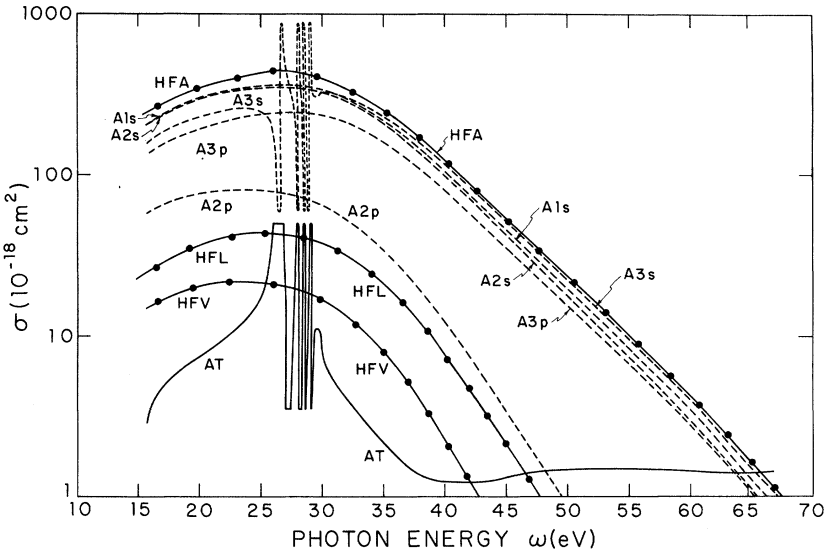

FIG. 2. $3p \rightarrow kd\ ^1P$ photoionization cross section for argon. The curves labeled HFL, HFV, and HFA are the lowest-order Hartree-Fock results using the length, velocity, and acceleration forms, respectively. Experiment is bracketed (Ref. 21) by the HFL and HFV curves. The acceleration-form curves labeled Ans ($n=1, 2, 3$) or Anp ($n=2, 3$) are obtained by adding that particular subshell's correlations to the lowest-order HFA result. The curve AT is the sum total of all first-order Coulomb correlations using the acceleration form. The $3s3p^6np\ ^1P$ autoionization resonances (with half-widths) are included in A3s and AT. The heights of the resonances have been truncated so as to avoid confusion in the figure.

ponents affect the lowest-order HFA result. The correlations with the $2p$ shell in the acceleration form have the largest first-order effect. Contributions from the components $[3p \rightarrow kd,\ 3p \rightarrow n's,\ k's]$ and $[3p \rightarrow kd,\ 2p \rightarrow n's,\ k's]$ were found to be quite small and were not included in Table I. The A3s curve of Fig. 2 includes the $3s3p^6np\ ^1P$ autoionization resonances. Widths and level shifts are included in a manner similar to previous work.[17] Since the $3p \rightarrow ks\ ^1P$ cross section was found earlier[17] to contribute only about 10% to the total $3p$ photoionization cross section, it was not investigated here. The AT curve in Fig. 2 is the sum total in the acceleration form of contributions from all the subshells through first order in the Coulomb correlations. The poor agreement of AT with HFL, HFV, and experiment, and the fact that the $3s \rightarrow n'p\ ^1P$ resonances do not show the experimental absorption windows,[21] indicates that the perturbation expansion in the acceleration form does not have good convergence properties for the argon $3p \rightarrow kd\ ^1P$ photoionization cross section. This is to be expected since the lowest-order acceleration result is so far from the correct value.

The $3s \rightarrow kp\ ^1P$ photoionization cross-section results are shown in Table I and Figs. 3 and 4. The experimental $3s$ removal energy (1.075 a.u.)[22] is used instead of the Hartree-Fock energy (1.278 a.u.), so that the threshold for photoionization of the $3s$ subshell occurs at the correct energy. The disparity in the HFL, HFV, and HFA curves for the $3s \rightarrow kp\ ^1P$ cross section of Fig. 3 is even larger than that found for the $3p \rightarrow kd\ ^1P$ cross section of Fig. 2. First-order correlations with the $2p$ shell again make the largest contributions to the lowest-order acceleration result. The Ans and Anp curves of Fig. 3 have the same meaning as those of Fig. 2 except we are now dealing with the $3s \rightarrow kp\ ^1P$ cross section. The curves labeled LT, VT, and AT in Fig. 3 include contributions to the $3s \rightarrow kp\ ^1P$ result from all subshells through first order in the Coulomb correlations. The curves labeled HFL, HFV, LT, and VT of Fig. 3 are repeated in Fig. 4 to show their agreement with a previous calculation by Amus'ya[1] and recent experimental results of Samson and Gardner.[23] Although the first-order correlated acceleration result AT is about 20 times experiment at threshold, it does possess the general shape of the length- and velocity-correlated curves and experiment.

The $2p \rightarrow kd\ ^1P$ photoionization cross-section results are shown in Table I and Fig. 5. The experimental $2p$ removal energy (9.156 a.u.)[22] is used instead of the Hartree-Fock energy (9.572 a.u.). The lowest-order HFL, HFV, and HFA curves agree moderately well. When first-order correlations are added, the agreement between the

TABLE I. Comparison of first-order subshell correlation effects on length, velocity, and acceleration matrix elements.

	M_L [a] (length)	M_V (velocity)	M_A (acceleration)
$3p \rightarrow kd\ ^1P$ photoionization at $\omega = 20.060$ eV			
HF[$3p \rightarrow kd$] [b]	1.7391	1.2950	5.3455
[$3p \rightarrow kd$, $3p \rightarrow n'd$, $k'd$] [c]	−0.2185	0.2050	−1.5929
[$3p \rightarrow kd$, $3s \rightarrow n'p$, $k'p$]	0.0147	0.0192	−0.7133
[$3p \rightarrow kd$, $2p \rightarrow n'd$, $k'd$]	−0.0062	−0.0091	−2.8165
[$3p \rightarrow kd$, $2s \rightarrow n'p$, $k'p$]	−0.0006	−0.0010	−0.4314
[$3p \rightarrow kd$, $1s \rightarrow n'p$, $k'p$]	0.0000	0.0000	−0.4201
Total	1.5285	1.5091	−0.6287
$3s \rightarrow kp\ ^1P$ photoionization at $\omega = 34.555$ eV			
	M_L [a] (length)	M_V (velocity)	M_A (acceleration)
HF[$3s \rightarrow kp$] [b]	0.1952	0.1808	2.7660
[$3s \rightarrow kp$, $3p \rightarrow n'd$, $k'd$] [c]	−0.5361	−0.3561	0.6678
[$3s \rightarrow kp$, $3s \rightarrow n'p$, $k'p$]	−0.0028	0.0034	−0.0440
[$3s \rightarrow kp$, $2p \rightarrow n'd$, $k'd$]	0.0104	0.0075	−1.8945
[$3s \rightarrow kp$, $2s \rightarrow n'p$, $k'p$]	0.0011	0.0060	−0.3703
[$3s \rightarrow kp$, $1s \rightarrow n'p$, $k'p$]	0.0000	0.0007	−0.6689
IM[$3s \rightarrow kp$, $3p \rightarrow k'd$] [d]	0.2188	0.1359	0.7515
Total (real) [e]	−0.3322	−0.1577	0.4561
Total (imaginary)	0.2188	0.1359	0.7515
$2p \rightarrow kd\ ^1P$ photoionization at $\omega = 262.743$ eV			
	M_L [a] (length)	M_V (velocity)	M_A (acceleration)
HF[$2p \rightarrow kd$] [b]	2.2991	2.2311	2.9685
[$2p \rightarrow kd$, $3p \rightarrow n'd$, $k'd$] [c]	0.0323	0.0096	−0.0510
[$2p \rightarrow kd$, $3s \rightarrow n'p$, $k'p$]	−0.0156	−0.0132	−0.0084
[$2p \rightarrow kd$, $2p \rightarrow n'd$, $k'd$]	−0.0602	0.0962	−0.2531
[$2p \rightarrow kd$, $2s \rightarrow n'p$, $k'p$]	0.0190	0.0292	−0.0519
[$2p \rightarrow kd$, $1s \rightarrow n'p$, $k'p$]	−0.0011	−0.0013	−0.2415
IM[$2p \rightarrow kd$, $3p \rightarrow k'd$] [d]	0.0163	0.0146	0.0180
IM[$2p \rightarrow kd$, $3s \rightarrow k'p$]	−0.0057	−0.0054	−0.0030
Total (real) [e]	2.2735	2.3516	2.3626
Total (imaginary)	0.0106	0.0092	0.0150

[a] M_L, M_V, and M_A are defined in Eqs. (8)–(10).

[b] Hartree-Fock approximation, lowest-order diagram Fig. 1(a).

[c] Angular-momentum component of first-order Coulomb correlation diagrams, Figs. 1(b) and (c), and their exchanges, real part (see notation explanation in text).

[d] Angular-momentum component of first-order Coulomb correlation diagrams, imaginary part.

[e] Cross section is obtained from squaring real part, squaring imaginary part, and adding.

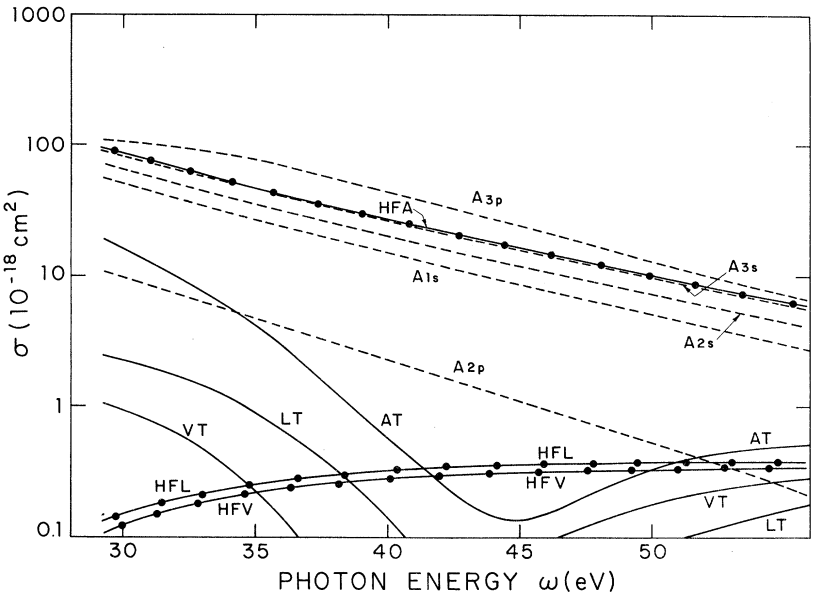

FIG. 3. $3s \rightarrow kp\ ^1P$ photoionization cross section for argon. The HFL, HFV, and HFA curves are the lowest-order Hartree-Fock results, while the LT, VT, and AT curves include all first-order Coulomb correlations using the length, velocity, and acceleration forms, respectively. The Ans and Anp curves have the same meaning as those of Fig. 2, except applied to a $3s \rightarrow kp\ ^1P$ photoionization process.

three forms LT, VT, and AT and the experimental points of Lukirskii and Zimkina[24] is quite good.

It has been shown above that the acceleration form of the dipole operator gives very poor results when it is used to calculate low-energy Hartree-Fock photoabsorption cross sections for argon. Only for the $2p \rightarrow kd\ ^1P$ cross section, which has an ionization threshold at 249.14 eV, does the lowest-order Hartree-Fock acceleration form agree somewhat with the length and velocity forms. The effects of first-order Coulomb correlations on the acceleration form for the $3p \rightarrow kd\ ^1P$ and $3s \rightarrow kp\ ^1P$ cross sections were found to be enormous. After including first-order correlations the acceleration results for the $3p \rightarrow kd\ ^1P$ cross section were still in quite poor agreement with experiment. Slow convergence of the perturbation expansion was also found in the $3s \rightarrow kp\ ^1P$ acceleration results, although the qualitative shapes of the three correlated forms and experiment were similar. For the high-energy $2p \rightarrow kd\ ^1P$ cross section all three forms were brought into

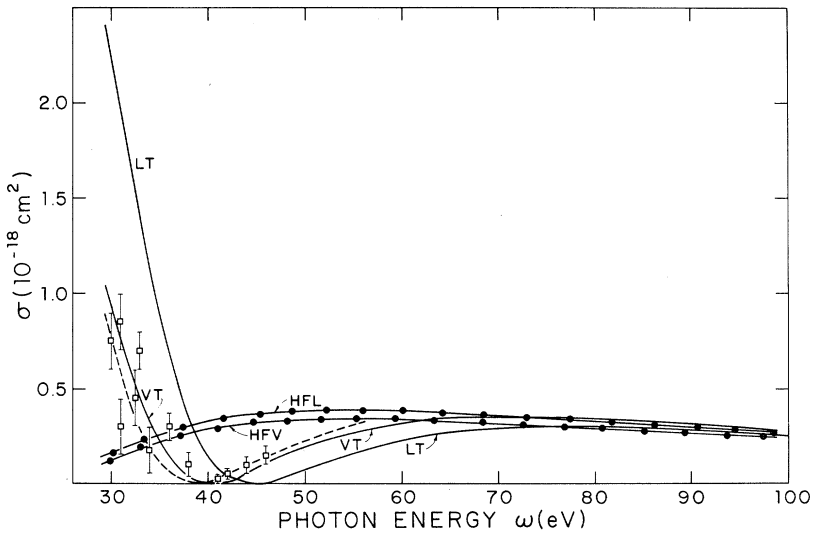

FIG. 4. $3s \rightarrow kp\ ^1P$ photoionization cross section for argon. The curves HFL and HFV are the Hartree-Fock length and velocity results, while LT and VT show the effects of adding first-order Coulomb correlations (same results as shown in Fig. 3). The dashed line is an earlier theoretical calculation by Amus'ya (Ref. 1) using the RPA. The experimental points are those of Samson and Gardner (Ref. 23).

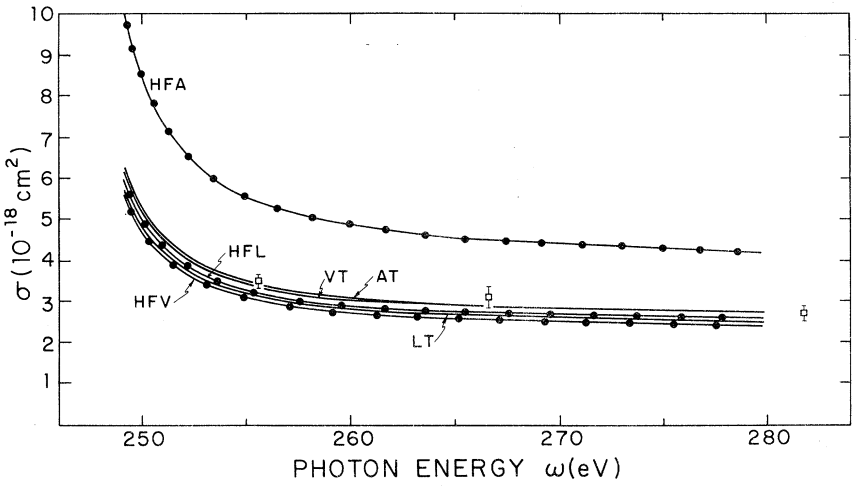

FIG. 5. $2p \rightarrow kd\,^1P$ photoionization cross section for argon. The HFL, HFV, and HFA curves are the Hartree-Fock results, while the LT, VT, and AT curves include first-order Coulomb correlations to the length, velocity, and acceleration forms, respectively. The experimental points are those of Lukirskii and Zimkina (Ref. 24).

good agreement with experiment by including first-order Coulomb correlations.

It can be concluded that, when using the acceleration form for the accurate calculation of photoabsorption processes in complex atoms, extreme caution must be applied. Comparison with the length and velocity forms should always be made.

We wish to thank Professor P. K. Kabir for a helpful discussion.

*Research supported by the National Science Foundation.

[1]M. Ya. Amus'ya, in *Invited Lectures and Progress Reports, Eighth International Conference on the Physics of Electron-Atom Collisions, Belgrade* (Institute of Physics, Belgrade, 1973), p. 171.

[2]V. P. Myerscough and G. Peach, in *Case Studies in Atomic Collision, Physics II* (North-Holland, Amsterdam, 1972), p. 293.

[3]G. V. Marr, *Photoionization Processes in Gases* (Academic, New York, 1967).

[4]R. P. Johnston, J. Quant. Spectrosc. Radiat. Transfer 7, 815 (1967).

[5]S. Chandrasekhar, Astrophys. J. 102, 223 (1945).

[6]A. L. Stewart, Proc. Phys. Soc. Lond. A 67, 917 (1954).

[7]A. L. Stewart, in *Advances in Atomic and Molecular Physics* (Academic, New York, 1967), Vol. 3, p. 1.

[8]U. Fano and J. W. Cooper, Rev. Mod. Phys. 40, 441 (1968).

[9]S. Geltman, J. Quant. Spectrosc. Radiat. Transfer 13, 601 (1973).

[10]J. L. Stilley and J. Callaway, Astrophys. J. 160, 245 (1970).

[11]H. P. Kelly, in Ref. 1, p. 239.

[12]K. A. Brueckner, Phys. Rev. 97, 1353 (1955).

[13]J. Goldstone, Proc. R. Soc. Lond. A 239, 267 (1957).

[14]M. Ya. Amus'ya, N. A. Cherepkov, and L. V. Chernysheva, Zh. Eksp. Teor. Fiz. 60, 160 (1971) [Sov. Phys.—JETP 33, 90 (1971)].

[15]H. P. Kelly and A. Ron, Phys. Rev. A 5, 168 (1972).

[16]H. A. Bethe and E. E. Salpeter, *Quantum Mechanics of One- and Two-Electron Atoms* (Springer-Verlag, Berlin, 1957).

[17]H. P. Kelly and R. L. Simons, Phys. Rev. Lett. 30, 529 (1973).

[18]C. E. Moore, *Atomic Energy Levels*, Natl. Bur. Std. Circ. No. 467 (U.S. GPO, Washington, D.C., 1949).

[19]H. J. Silverstone and M. L. Yin, J. Chem. Phys. 49, 2026 (1968).

[20]S. Huzinaga and C. Arnau, Phys. Rev. A 1, 1285 (1970).

[21]R. P. Madden, D. L. Ederer, and K. Codling, Phys. Rev. 177, 136 (1969).

[22]K. Siegbahn *et al.*, Nova Acta Regiae Soc. Sci. Upsal. 20, 1 (1967).

[23]J. A. R. Samson and J. L. Gardner, Phys. Rev. Lett. 33, 671 (1974).

[24]A. P. Lukirskii and T. M. Zimkina, Bull. Acad. Sci. USSR, Phys. Ser. 27, 808 (1963).